Pergamon

Geochimica et Cosmochimica Acta Vol 58 No 24 pp 5465–5478 1994

0016 7037/94 $6 00 + 00

0016-7037(94)00341-6

Uranium(VI) adsorption to ferrihydrite Application of a surface complexation model

T D WAITE [1]* J A DAVIS [2] T E PAYNE [1] G A WAYCHUNAS [3] and N XU [3]

[1]Australian Nuclear Science and Technology Organisation Environmental Science Program
Private Mail Bag 1 Menai NSW 2234 Australia
[2]United States Geological Survey Water Resources Division 345 Middlefield Road MS-465 Menlo Park CA 94025 USA
[3]Center for Materials Research, Stanford University Stanford CA 94305 USA

(*Received March* 14 1994 *accepted in revised form August* 25 1994)

Abstract—A study of U(VI) adsorption by ferrihydrite was conducted over a wide range of U(VI) concentrations pH and at two partial pressures of carbon dioxide A two-site (strong- and weak-affinity sites $\equiv Fe_sOH$ and $\equiv Fe_wOH$ respectively) surface complexation model was able to describe the experimental data well over a wide range of conditions with only one species formed with each site type an inner-sphere mononuclear, bidentate complex of the type $(\equiv FeO_2)UO_2$ The existence of such a surface species was supported by results of uranium EXAFS spectroscopy performed on two samples with U(VI) adsorption density in the upper range observed in this study (10 and 18% occupancy of total surface sites) Adsorption data in the alkaline pH range suggested the existence of a second surface species modeled as a ternary surface complex with $UO_2CO_3^0$ binding to a bidentate surface site Previous surface complexation models for U(VI) adsorption have proposed surface species that are identical to the predominant aqueous species e g multinuclear hydrolysis complexes or several U(VI)-carbonate complexes The results demonstrate that the speciation of adsorbed U(VI) may be constrained by the coordination environment at the surface giving rise to surface speciation for U(VI) that is significantly less complex than aqueous speciation

INTRODUCTION

THE MOBILITY OF U in water-rock systems is dependent both upon its ability to form insoluble precipitates and particularly at relatively low total uranium concentrations upon its tendency to adsorb to solid substrates Considerable advances have been made in developing a coherent set of thermodynamic data for describing the solution and mineral equilibrium behaviour of U (GRENTHE et al 1992) but despite an extensive range of investigations of the adsorption behaviour of uranium (reviewed in WAITE et al 1994) considerable uncertainty still remains concerning the best approach to model uranium adsorption to mineral phases

Figures 1 and 2 show the complex distribution of U(VI) aqueous species as a function of pH in the absence of carbonate and at equilibrium with two different partial pressures of CO_2 The calculations were made with the equilibrium speciation computer code HYDRAQL (PAPELIS et al, 1988) using the thermodynamic data given in Table 1 The stability of well-crystallized β-$UO_2(OH)_2$ in the absence of carbonate is illustrated in Fig 1a the aqueous speciation is dominated by mononuclear U(VI) species at all pH values in this system but the multinuclear species $(UO_2)_2(OH)_2^{2+}$ and $(UO_2)_3(OH)_5^+$ are also important At low total dissolved U(VI) concentrations ($<10^{-8}$ M), these multinuclear species are much less important (Fig 1b) If it is assumed that the precipitation of β-$UO_2(OH)_2$ is kinetically hindered and the solubility is controlled by an amorphous phase multinuclear species can predominate at higher total dissolved U(VI) concentrations (Fig 1c) However, in equilibrium with air aqueous speciation of U(VI) in the neutral to alkaline pH range is dramatically influenced by the formation of strong carbonate complexes (Fig 2a) Different species predominate at different partial pressures of CO_2 (Fig 2b)

Qualitative observations of U(VI) sorption have been reported for a large range of single and complex substrates For example STARIK et al (1958) studied the sorption of trace concentrations of U(VI) to Fe oxyhydroxides and found adsorption to be greatest at a pH of approximately 5 Uranium(VI) adsorption decreased in the presence of carbonate TRIPATHI (1983) and HSI and LANGMUIR (1985) found that carbonate played a critical role in the distribution of U(VI) between the surfaces of Fe oxide phases and solution They observed that at higher carbonate concentrations when the $UO_2(CO_3)_2^{2-}$ and $UO_2(CO_3)_3^{4-}$ species dominate in solution (Fig 2) there was a sharp decrease in the extent of U(VI) adsorption with a resultant high-pH or desorption' edge TRIPATHI (1983) found that very high U(VI) adsorption was observed under conditions where $(UO_2)_2CO_3(OH)_3^-$ was the predominant U(VI) aqueous species

Similar results were found by Ho and coworkers for U(VI) sorption on hematite (HO and DOERN 1985, HO and MILLER, 1986) and magnetite (SAGERT et al, 1989) These authors were interested in the identity of the adsorbed uranyl species particularly in the presence of carbonate Based on the electrophoretic mobility of particles with adsorbed U(VI), Ho and coauthors concluded as did TRIPATHI (1983) that $(UO_2)_2CO_3(OH)_3^-$ was an important adsorbing species when carbonate is present HO and DOERN (1985) suggested that $(UO_2)_3(OH)_5^+$ was the major U(VI) adsorbing species in the absence of carbonate

A number of authors have applied the surface complexation approach to modelling the partitioning of U(VI) between

* *Present address* Department of Water Engineering University of New South Wales Sydney NSW 2052 Australia

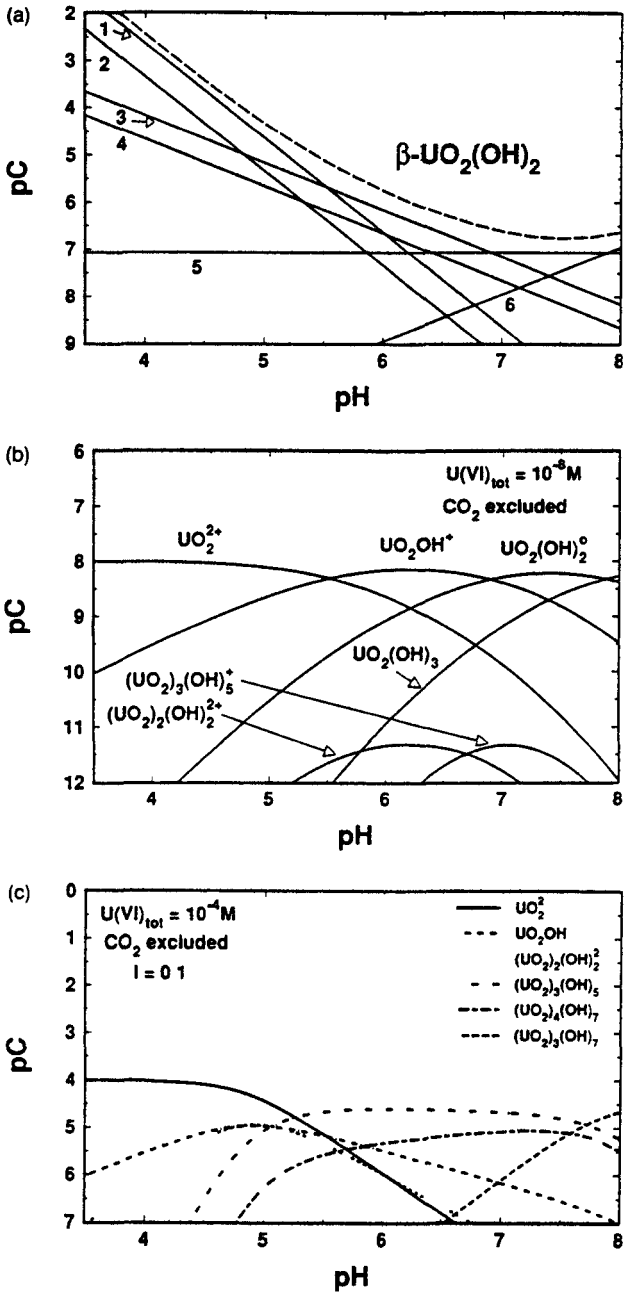

FIG 1 Distribution of major U(VI) species in the absence of CO_2 (I = 0 1) pC (−log concentration) of species as a function of pH (a) Solubility of β-$UO_2(OH)_2$ showing dominant species as a function of pH 1 UO_2^{2+} 2 $(UO_2)_2(OH)_2^{2+}$ 3 UO_2OH^+, 4 $(UO_2)_3(OH)_5^+$ 5 $UO_2(OH)_2^0$ 6 $UO_2(OH)_3^-$ (b) Speciation of U(VI) at a total dissolved concentration of 10^{-6} M (c) Speciation of U(VI) at a total dissolved concentration of 10^{-4} M precipitation of crystalline U(VI) oxides prohibited in the calculation

solid and solution phases over the last ten years The basic modelling approach has been similar in each case, with minor differences in the mode of description of the electrical double layer and more importantly differences in the proposed surface complexes For example HSI and LANGMUIR (1985) used the triple layer model of DAVIS et al (1978) to describe their experimental results as a function of pH and dissolved carbonate They assumed that the dominant aqueous phase species UO_2OH^+ and $(UO_2)_3(OH)_5^+$ were adsorbed in the absence of carbonate and found good agreement between the experimental results and model simulations using the following surface complexation reactions

$$\equiv FeOH + UO_2^{2+} + H_2O \leftrightarrow \equiv FeO^- - UO_2OH^+ + 2H^+ \quad (1)$$

and

$$\equiv FeOH + 3UO_2^{2+} + 5H_2O \leftrightarrow \equiv FeO^- - (UO_2)_3(OH)_5^+ + 6H^+ \quad (2)$$

where ≡FeOH represents an hydroxyl functional group on the surface and the left-hand side of the equations are written in terms of system components rather than the predominant aqueous species (DZOMBAK and MOREL 1990) The possibility of formation of bidentate and tridentate surface complexes was also considered by HSI and LANGMUIR (1985) with a bidentate complex of the form $(\equiv FeO^-)_2 - (UO_2)_3(OH)_5^+$ (in conjunction with $\equiv FeO^- - UO_2OH^-$) fitting the data as well as Eqn 2

In the presence of carbonate HSI and LANGMUIR (1985) found it necessary to assume the formation of strong U(VI)

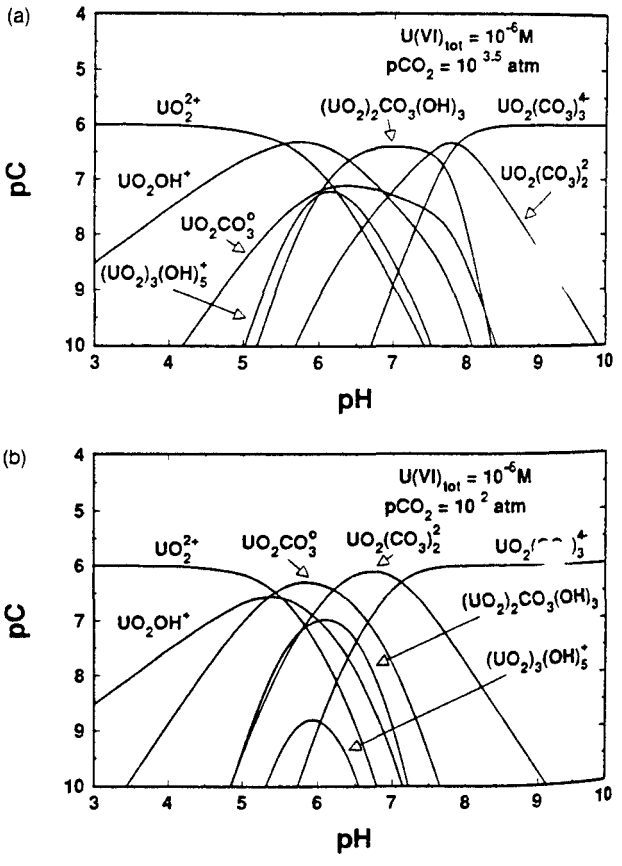

FIG 2 Dissolved speciation of U(VI) at a total concentration of 10^{-6} M in an open system equilibrated with (a) a partial pressure of CO_2 of $10^{-3.5}$ atm or (b) a partial pressure of CO of 10^{-2} atm Ionic strength = 0 1 pC (−log concentration) of species as a function of pH

Table 1 U(VI) Aqueous Phase Reactions[a]

Reaction	logK (I=0)
$UO_2^{2+} + OH^- = UO_2OH^+$	8 8
$UO_2^{2+} + 2OH^- = UO_2(OH)_2^0$	16 0
$UO_2^{2+} + 3OH^- = UO_2(OH)_3^-$	22 0
$UO_2^{2+} + 4OH^- = UO_2(OH)_4^{2-}$	23 0
$2UO_2^{2+} + OH^- = (UO_2)_2(OH)^{3+}$	11 2
$2UO_2^{2+} + 2OH^- = (UO_2)_2(OH)_2^{2+}$	22 37
$3UO_2^{2+} + 4OH^- = (UO_2)_3(OH)_4^{2+}$	44 1
$3UO_2^{2+} + 5OH^- = (UO_2)_3(OH)_5^+$	54 44
$3UO_2^{2+} + 7OH^- = (UO_2)_3(OH)_7^-$	67 0
$4UO_2^{2+} + 7OH^- = (UO_2)_4(OH)_7^+$	76 1
$UO_2^{2+} + CO_3^{2-} = UO_2CO_3^0$	9 7
$UO_2^{2+} + 2CO_3^{2-} = UO_2(CO_3)_2^{2-}$	17 0
$UO_2^{2+} + 3CO_3^{2-} = UO_2(CO_3)_3^{4-}$	21 63
$2UO_2^{2+} + CO_3^{2-} + 3OH^- = (UO_2)_2CO_3(OH)_3^-$	40 82[b]
$\beta\ UO_2(OH)_2 = UO_2^{2+} + 2OH^-$	23 07

[a]Stability constants from Grenthe et al (1992)
[b]Stability constant from Tripathi (1983)

carbonate complexes at the surface in order to fit their adsorption data They assumed that the dominant solution phase species was the dominant adsorbing species i e writing the left-hand side of the equations in terms of components again

$$\equiv FeOH + UO_2^{2+} + 2CO_3^{2-} + H^+ \leftrightarrow \equiv FeOH_2^+-UO_2(CO_3)_2^{2-} \quad (3)$$

and

$$\equiv FeOH + UO_2^{2+} + 3CO_3^{2-} + H^+ \leftrightarrow \equiv FeOH_2^+-UO_2(CO_3)_3^{4-} \quad (4)$$

By considering these additional surface species Hsi and Langmuir (1985) were able to obtain excellent agreement between model simulations and U(VI) adsorption data on goethite for a single total inorganic C content ($C_T = 10^{-2}$ M) However, the model simulations were less successful in descr ig adsorption data for $C_T = 10^{-3}$ M

Pa E and Waite (1991) applied the proposed model of Hsi and Langmuir (1985), including the same reaction set and stability constants to model U(VI) sorption on the amorphous Fe oxide component of a weathered schist These authors found poor agreement between model simulations and their experimental data At the total carbonate concentrations used in their study (2 mM), the $UO_2CO_3^0$ aqueous species was important in the pH range 4 8–6 4 and the fit of the model simulations to the data were greatly improved when was assumed that a $\equiv FeO^-$–$UO_2CO_3^0$ surface complex med

In the applications of surface complexation models to describe U(VI) adsorption by iron oxides investigators have usually assumed that the predominant aqueous species are involved in surface complex formation Because U(VI) aqueous speciation is complex this has led to a wide range of proposed surface species and a unified approach to the modeling is lacking Major differences among the modeling approaches include (1) the most appropriate choice of surface species at low pH where complexation by carbonate is unimportant and (2) the number type and presumed importance of U(VI)-carbonate-surface ternary complexes Although polynuclear U(VI) species are known to be thermodynamically stable in aqueous solution (Figs 1 2) the likelihood of polynuclear species at the surface, e g $\equiv FeO^-$–$(UO_2)_3(OH)_5^+$, has not been tested in adsorption studies by a systematic variation of the total U(VI) concentration Although surface species should ideally be identified by spectroscopic methods detection limit problems make it difficult to confirm bonding structures at low U(VI) concentrations

In this paper we report the results of studies of U(VI) adsorption on ferrihydrite over a wide range of solution and suspension conditions In addition to the batch experiments U Extended X-ray Absorption Fine Structure (EXAFS) data were collected and analyzed for two ferrihydrite samples with high adsorption density A surface complexation model with simple surface speciation is used to describe the adsorption data Both the surface complexation model and the results of X-ray absorption spectroscopy suggest that the species formed is a unique product of the coordination environment at the surface which is independent of the predominant U(VI) species in solution

EXPERIMENTAL

Materials

Ferrihydrite is a microcrystalline hydrous Fe oxide that may exhibit a number of different crystalline phases with a stoichiometry near $Fe_2O_3 \cdot H_2O$ (Towe and Bradley 1967 Schwertmann and Fischer 1973 Manceau et al 1990 Waychunas et al 1993 Rea et al 1994) The least crystalline form of ferrihydrite displays two broad X ray diffraction peaks indicating poor structural order and small particle size and has been referred to as two line ferrihydrite (Schwertmann and Fischer 1973 Murad and Schwertmann 1980) Two-line ferrihydrite was precipitated by raising the pH of a Fe^{3+}/HNO_3 solution to 6 0 and then aged for 65 h at pH 6 and 25°C in a continuously stirred pH and temperature-controlled vessel

The elementary unit of the ferrihydrite structure is an Fe^{3+} ion surrounded by six close packed O^{2-} or OH^- anions i e an Fe octahedron (Waychunas et al 1993) Larger units consist of the Fe octahedra joined by sharing edges forming short double chains of octahedra these link further to other chains by sharing corners to form a cross linked structure similar to goethite or akaganeite (Waychunas et al 1993) Electron micrographs indicate spherical crystal morphology (Schwertmann and Taylor 1977) but these particle are expected to be comprised of large aggregates of the cross-linked dioctahedral chains (Waychunas et al 1993) The primary particle size is believed to consist of 15–40 A spheres (Murphy et al 1976a b Dousma and de Bruyn 1976) but wide angle X ray scattering studies suggest a crystallite coherence length of 8–15 A (Waychunas et al 1994)

A primary U(VI) stock solution (10 000 mg U/L) in 10% HNO_3 was prepared from analytical grade uranyl nitrate solution A secondary stock (59 mg U/L) prepared in 0 01 M HNO_3 was prepared for addition of aliquots to batch adsorption experiments For batch experiments with very dilute total U(VI) concentrations (10^{-7} M or less) a ^{236}U isotope was used as a radiotracer The ^{236}U was obtained from the Chemistry Division of the U K Atomic Energy Authority (Harwell) as a standard solution in 2 M nitric acid All other chemicals used were reagent grade

Batch Experiments

Aliquots of the aged ferrihydrite slurry were transferred to open polypropylene centrifuge tubes and sufficient $NaNO_3$ was added to bring the suspensions to the desired ionic strength (always 0.1 M $NaNO_3$, except in the ionic strength dependence experiments). Concentrations of ferrihydrite used were 10^{-3} M (as Fe) in most of the batch studies. For studies at pH > 7.0 sufficient $NaHCO_3$ was added to achieve equilibrium with air at the desired experimental pH. The pH of the slurry was adjusted to the desired experimental value immediately before and after $NaHCO_3$ addition and the tube was shaken for 24 h in a water bath at 25°C. Several 2-mm holes were drilled in the centrifuge tube lids in order to keep the system open to the atmosphere. At the end of the 24 h period the pH was remeasured but not adjusted. pH drift was always less than 0.15 pH units. The desired amount of U(VI) was then added (usually 10^{-6} M except in the studies of dependency on total U concentration) with immediate readjustment of the pH to the value measured just prior to U(VI) addition. With the exception of the study of adsorption kinetics the precipitate and aqueous phases were separated by centrifugation after 48 h of mixing. The pH was measured again at the time of sampling. The dissolved U concentration was typically determined by kinetic phosphorescence analysis (discussed below) except in cases where very low concentrations of U(VI) were added. In these experiments the artificial isotope ^{236}U was added and adsorption was quantified by isotopic dilution using alpha-spectrometry (see below).

While most of the experiments were conducted under atmospheric conditions, some investigations were performed in a glove box at an elevated partial pressure of carbon dioxide. The gas composition used in the glovebox was a 50:50 mixture of ordinary air with a 2% CO_2/98% N_2 special gas mixture yielding a final gas composition of 1% CO_2/10% O_2/89% N_2.

Analytical Methods for Dissolved U(VI)

The U(VI) concentration of the supernatant was determined in most experiments with a kinetic phosphorescence analyser (model KPA-10 Chemchek Instruments, Richland, WA). In practice a detection limit of about 10^{-9} M U(VI) can be readily achieved and even lower detection limits are achieved when minor interfering substances e.g. chloride are absent from the sample. Comparison with results obtained by alpha-spectrometry and inductively coupled plasma-mass spectrometric analysis confirmed that the kinetic phosphorescence analyser (KPA) results were accurate to within ±3%.

Alpha spectrometry was used for the determination of U(VI) when the concentration in solution was below the detection limit of the KPA technique. In these instances 10^{-7} M or 10^{-8} M of the artificial isotope ^{236}U (rather than natural U) was added to the batch experiments. A known quantity of ^{232}U (another artificial isotope) was added to supernatant samples as a yield tracer. After standard chemical separation steps (PAYNE and WAITE, 1991) the uranium isotope activities were measured using an Ortec Alpha-King alpha-spectrometer and the concentration of ^{236}U in solution was determined from the relative count rates of ^{232}U and ^{236}U.

X-Ray Absorption Spectrometry

EXAFS data were collected on the U L_{III} edge over the energy range 17,100–18,160 eV at the Stanford Synchrotron Radiation Laboratory (SSRL) on beamline 4-1 using Si (111) monochromator crystals. Samples were held within milled slots in 4 mm thick Teflon plates. Kapton tape over the slots held the sample pastes in place. Fluorescence yield spectra were collected under ambient conditions using an Ar-filled ion chamber with soller slit and Sr filter assembly to limit scattered radiation (STERN and HEALD, 1979). Transmission spectra were collected for a solid model compound uraninite (UO_2). Minimal (5%) detuning of the monochromator was necessary to remove beam harmonics.

Samples for EXAFS data collection were prepared in the same manner as that used in the batch adsorption experiments, and then were concentrated as wet pastes. 2 L batches of ferrihydrite (10^{-3} M as Fe) were precipitated by raising the pH of a Fe^{3+}/HNO_3 solution to 6.0 and then aged for 65 h at pH 6 and 25°C in a continuously stirred pH and temperature-controlled vessel. Sufficient $NaNO_3$ was added to bring the suspensions to an ionic strength of 0.1 M $NaNO_3$. The pH of the slurries were then adjusted to pH 5 (sample UF3) or 5.5 (sample UF4) and held constant at the selected pH values for 24 h. Uranium(VI) was then added to a concentration of 10^{-4} M, the suspension was mixed at constant pH for 48 h and then was concentrated to a wet paste by centrifugation. U/Fe molar ratios in the precipitates were 0.044 and 0.077 respectively for samples UF3 and UF4.

RESULTS AND DISCUSSION

The concentration of dissolved U(VI) measured in batch experiments decreased rapidly within the first few hours indicating a rapid initial adsorption process (Fig. 3). Subsequently, a slower sorption process that continued for at least 200 hours was observed. This type of sorption kinetics is typical for the binding of inorganic ions to ferrihydrite and other mineral surfaces (DAVIS and KENT, 1990). The rate of the initial adsorption process is probably controlled by film diffusion at the exterior of particles which takes only minutes to reach equilibrium if mass transport in the bulk solution is not limiting. FULLER et al. (1993) have shown that the slower process (for arsenate sorption) on ferrihydrite is due to diffusion into large aggregates formed by the ferrihydrite particles. We assume that a similar mechanism may account for the slow rate of U(VI) adsorption observed in our experiments. For all subsequent batch experiments with ferrihydrite, a reaction time of 48 h was chosen to approximate equilibrium since greater than 95% of the adsorption occurred within this reaction time.

Uranium(VI) adsorption to ferrihydrite (1 mM as Fe) as a function of pH and ionic strength in systems open to the atmosphere is shown in Fig. 4a. Adsorption increases from near zero at pH 3.5 to greater than 99% of the total U(VI) at pH 5.5 and then decreased to zero in the pH region 8–9. Similar observations have been made by HSI and LANGMUIR (1985), and the results suggest that U(VI) adsorption decreases in the weakly alkaline pH range due to the formation of aqueous U(VI)-carbonato complexes (Fig. 2). Within experimental error, U(VI) adsorption was independent of ionic

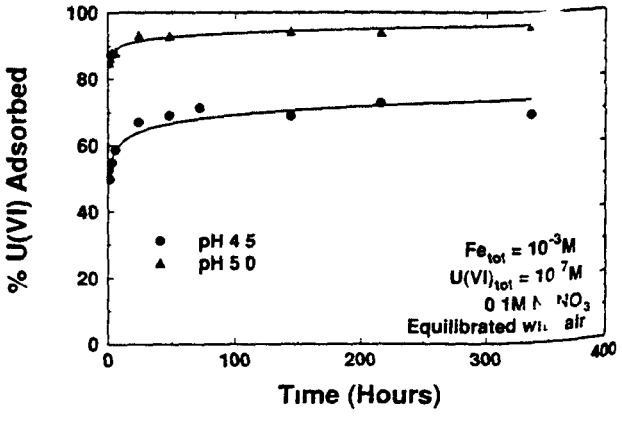

FIG. 3. Adsorption of 10^{-7} M U(VI) on ferrihydrite (10^{-3} M as Fe) in 0.1 M $NaNO_3$ as a function of time at pH 4.5 and 5.0. System open to the atmosphere.

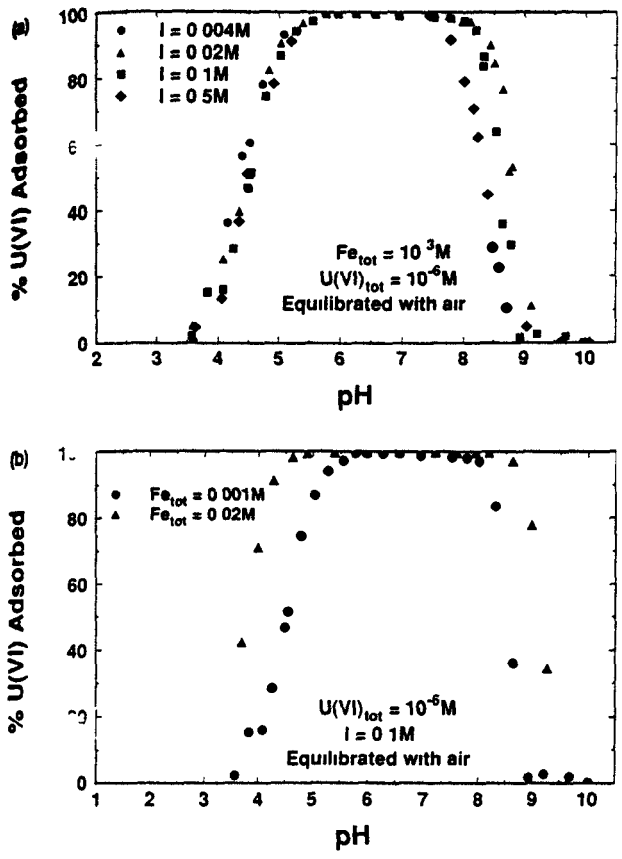

FIG 4 (a) Adsorption of 10^{-6} M U(VI) on ferrihydrite (10^{-3} M as Fe) as a function of pH and ionic strength System open to the atmosphere (b) Adsorption of 10^{-6} M U(VI) as a function of pH on two different concentrations of ferrihydrite (0 02 M or 0 001 M as Fe) in 0 1 M $NaNO_3$ System open to the atmosphere

strength in the acidic pH range but exhibited a slight dependence on ionic strength in alkaline solution Previous modeling studies of trace cation adsorption on hydrous oxides suggest that the formation of an inner-sphere surface complex is consistent with observations of adsorption that are independent of ionic strength (DAVIS and KENT 1990)

At a given pH, dissolved U(VI) decreased if additional ferrihydrite was present (Fig 4b) This result is expected if an adsorption reaction controls the dissolved U(VI) concentration since more surface sites are present when more ferrihydrite is added The result also confirms that the concentration of dissolved U(VI) was not controlled by the solubility of a U(VI) precipitate, since the addition of more ferrihydrite would not be expected to affect dissolved U(VI) in that case

The dependence of adsorption on the total U(VI) concentration in the batch experiments is shown in Fig 5 Adsorption data are shown for batch experiments with total U(VI) concentrations of 10^{-8} M, 10^{-6} M 10^{-5} M and 10^{-4} M in the acidic pH range and for 10^{-6} M and 10^{-4} M in the alkaline pH range The pH "edge" in the acidic pH range moved to a higher pH region as the total U(VI) concentration added was increased This trend in adsorption with increasing U(VI) concentration is opposite from that expected if polynuclear U(VI) complexes formed at the surface In solution multinuclear species increase in importance as the total dissolved U(VI) concentration increases (see Fig 1b c) because of the exponential dependence on UO_2^{2+} in the mass law equation for these species By analogy if a multinuclear U(VI) surface complex formed at the lower U(VI) concentrations the proportion of total U(VI) adsorbed at a given pH should increase as the U(VI) concentration increases (assuming surface sites in excess) Instead the proportion of total U(VI) adsorbed at a given pH decreases as the U(VI) concentration increases (Fig 5) This trend as a function of U(VI) concentration is consistent with that typically observed for transition metal cations (BENJAMIN and LECKIE, 1981) which are known to form mononuclear surface complexes (DAVIS and KENT 1990 CHISHOLM-BRAUSE et al 1990 ROE et al 1991)

The trend in adsorption with U(VI) concentration means that the average free energy of adsorption (per mole) decreases with increasing surface coverage Plotting the data obtained at pH 4 50 (±0 05) in isotherm form (log dissolved U(VI) vs log adsorbed U(VI)) results in a Freundlich isotherm with a slope of approximately 0 64 over four orders of magnitude in U(VI) concentration (WAITE et al 1994) This indicates that U(VI) adsorption was not proportional to the dissolved U concentration (i e the isotherm is nonlinear) Note also that the pH edge in the alkaline region shifted to a lower pH range in the batch experiments with higher U(VI) concentration This shift also implies a decrease in the average free energy of U(VI) adsorption with increasing surface coverage in the alkaline pH range

The pH dependence of U(VI) adsorption as a function of the partial pressure of CO_2 is illustrated in Fig 6 Increasing the partial pressure of CO_2 to 1% resulted in a very small increase in the proportion of U(VI) adsorbed in the acidic pH range but caused a significant decrease in U(VI) adsorption in the pH range 7–9 The effect is consistent with the hypothesis that the formation of aqueous U(VI)-carbonato complexes is responsible for the decrease in U(VI) adsorption observed in the alkaline pH range In a qualitative way the result can be viewed as a competition between the

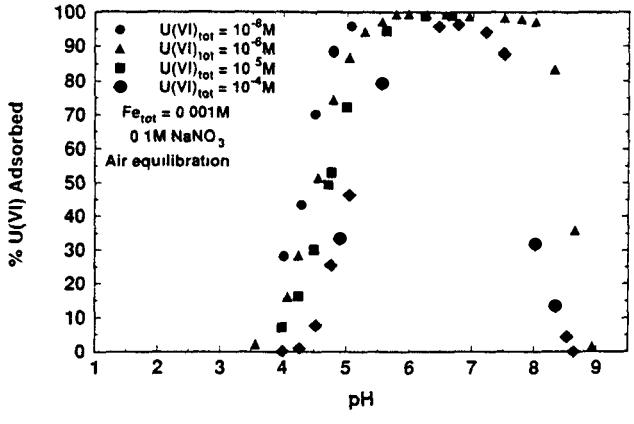

FIG 5 Adsorption of U(VI) on ferrihydrite (10^{-3} M as Fe) as a function of pH and total U(VI) concentration in 0 1 M $NaNO_3$ System open to the atmosphere

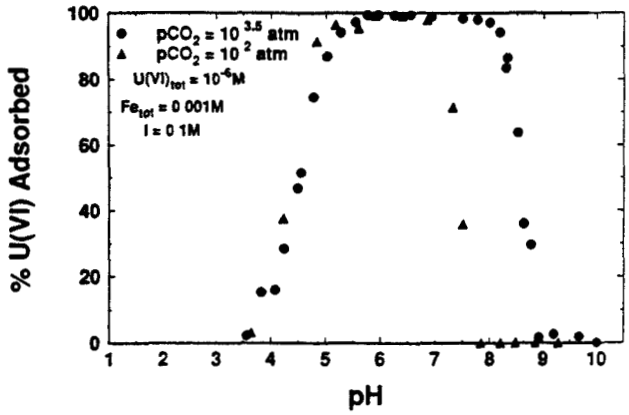

FIG 6 Adsorption of 10^{-6} M U(VI) on ferrihydrite (10^{-3} M as Fe) as a function of pH and partial pressure of CO_2 in 0 1 M $NaNO_3$

ferrihydrite surface and aqueous carbonate anions for coordination of the uranyl cation

EXAFS Data Analysis

X-ray absorption spectroscopy (XAS) was developed as a quantitative short-range structural probe during the 1970s and is applied increasingly in studies in the geosciences (BROWN 1990) XAS is an element-specific bulk method giving information about the average local structural and compositional environment of the absorbing atom In EXAFS the extended fine structure beyond an X-ray absorption edge yields structural information for an element after Fourier transformation of the fine structure (see review article by BROWN 1990) Because of the method of sample preparation in the current study U was present in significant quantities only at the surface of ferrihydrite Thus although EXAFS is a bulk technique its application here yielded structural information about adsorbed U(VI)

Because of the lack of availability of suitable model compounds we used the ab initio routine FEFF-5 03 (REHR et al , 1991, MUSTRE DE LEON et al , 1991) to calculate EXAFS phase and amplitude functions for U—O (axial and equatorial) U—Fe, and U—U atom absorber-backscatterer pairings Testing of similar FEFF-derived ab initio ph and amplitude functions for the U—O pairs had been do pre viously by a colleague in the fitting of many model compound spectra (H A Thompson, pers commun) Further testing of U—O and U—U phase and amplitude functions were done on our uraninite spectra In all cases, the fits were of excellent quality Separate phase and amplitude functions were necessary in all cases for the U—O axial and U—O equatorial pairs as the former contributes much more amplitude to the EXAFS spectrum No model compound spectra were available to test the calculated U—Fe function

Sample spectra were analyzed with the EXAFSP programs available at SSRL Figure 7 shows the extracted EXAFS signal from sample UF4 Though the signal is somewhat noisy well-defined EXAFS oscillations continue out to 16

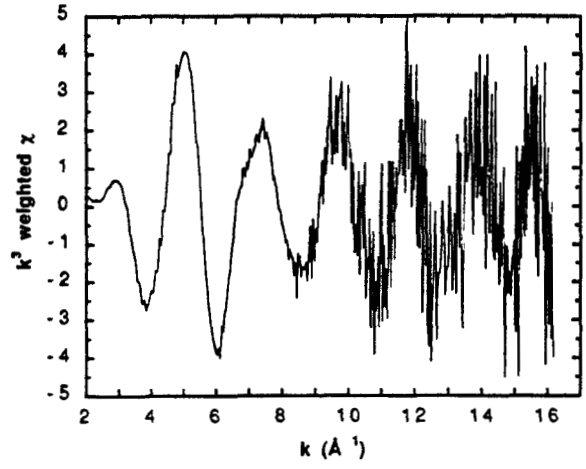

FIG 7 Extracted EXAFS spectrum from sample UF4 weighted by k^3

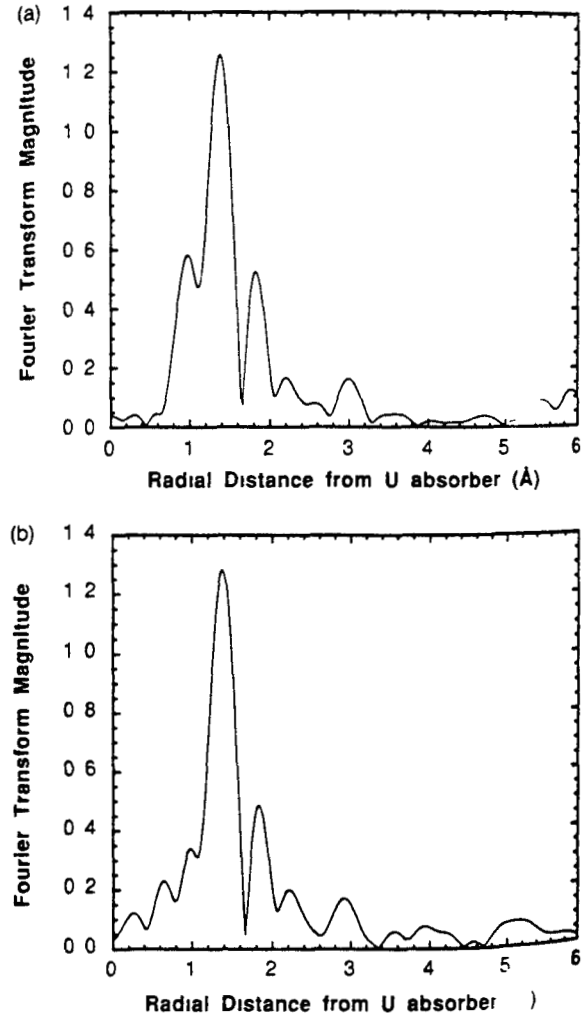

FIG 8 Fourier-transformed EXAFS spectra (EXAFS structure functions) for samples (a) UF3 and (b) UF4 The first four major peaks at circa 1 0 1 4 1 9 and 2 2 A are all due to U—O atom pair backscattering and the peak at circa 3 0 A is due to U—Fe atom pair backscattering

Å^{-1} Fourier transforms of the EXAFS spectra of samples UF4 and UF3 are shown in Fig 8 The first four-peak region of the Fourier transform (or EXAFS structure function) contains information on the various U—O bonds This region was backtransformed into k-space and fit with the FEFFderived functions (Fig 9a) Analogously the fifth peak near 3 Å which contains the U—Fe contributions, was backtransformed into k-space and fit (Fig 9b) Three U—O and one U—Fe shell were used to fit the data (U—O_{axial}, U—$O_{equatorial}$, U—$O_{sorbing}$, and U—Fe) Fits without the adsorbed (longest bond length) equatorial U—O pairs were notably poorer than fits that included this shell Also, a well-defined U—Fe shell was necessary for a reasonable fit particularly at higher k values

Besides filtering the separate EXAFS contributions in the EXAFS structure function for fitting we also fit the entire EXAFS function with four shells This produced very similar U—O results but slightly different U—Fe results However, as we discuss below, all fits are consistent with edge-sharing uranyl groups sorbed onto Fe oxyhydroxyl octahedra, i e , a mononuclear, bidentate sorption complex (Fig 10) The difference in the fits between full-pattern and filtered EXAFS is believed due to major U—O contributions that superimpose onto the U—Fe peak in the structure function, and which cannot be separated by filtering The fit results for sample UF3 are very similar to those for UF4 All results are shown in Table 2

Our results differ only slightly in bond distances and coordination numbers from those of MANCEAU et al (1992), as do our EXAFS spectra and structure functions This may be due to slight differences in sample preparation and also to the larger k-range of our data However, the U—Fe distances we obtain are quite similar Due to the relatively well-defined size of the uranyl group in crystal structures (e g , ABERG 1969 1970, 1971 ABERG et al 1983) we can postulate the U—Fe distance for idealized ferrihydrite-uranyl

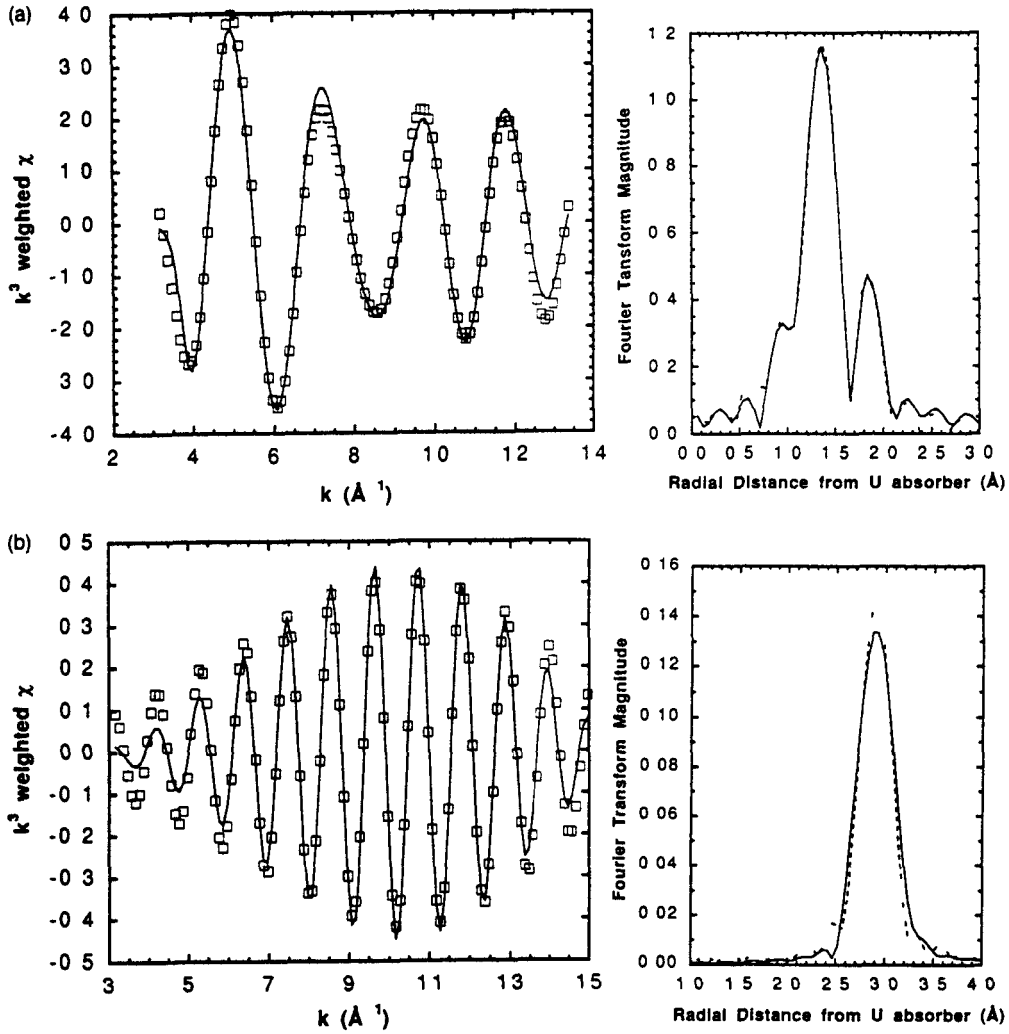

FIG 9 Fit to Fourier-filtered EXAFS contributions in sample UF4 from (a) U—O peak region of structure function over k-range 3 0–13 5 Å^{-1} (b) U—Fe peak region of structure function over k-range 3 0–15 0 A^{-1} Filtered data points are shown and the solid line is the fit model The Fourier transform of each fit is shown at the right The solid line is the transform of the fit and the dashed line represents the filtered data

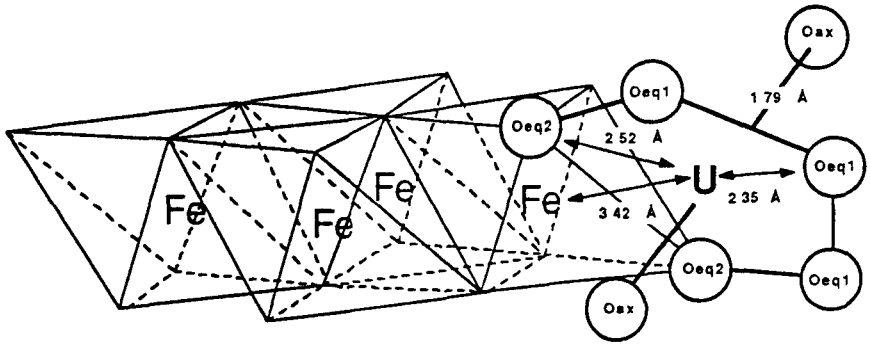

FIG 10 Model structure for the bidentate surface complex of UO_2^{2+} on ferrihydrite showing the edge sharing bond with an iron octahedron that is part of a dioctahedral chain O_{ax} represents axial oxygen atoms of UO_2^{2+} O_{eq1} represents equatorial oxygen atoms of UO_2^{2+} not involved in the complex and O_{eq2} represents equatorial oxygen atoms shared with the iron octahedron

bidentate sorption complexes These can share two uranyl equatorial oxygens with the adjacent apices of edge-sharing Fe oxyhydroxyl octahedra in several ways (see COMBES 1988) or there can be edge-sharing with a single Fe oxyhydroxyl octahedron In the former case the U—Fe distances are on the order of 4 2–4 3 Å or more and there are two Fe second neighbor ions contributing to the backscattering In the latter case there is a single Fe ion second neighbor to the U ion and the U—Fe distance is about 3 3–3 5 Å

All of our fits indicate only 0 4–1 1 Fe neighbors at a distance of 3 33–3 41 Å Attempts to fit U—U pairings for these distances showed poor agreement both in phase and amplitude U—U distances could also not be fit for any larger distances suggesting that either uranyl multinuclear complexes do not exist on the ferrihydrite surface or that the U—U backscattering makes only a negligible contribution to the EXAFS As our FEFF-5 03 calculations indicated a backscattering amplitude for U—U pairings in a hypothetical tetranuclear uranyl cluster (ABERG 1971) that was larger than that calculated separately for U—Fe backscatterers at 3 4 A we conclude that within the margin of detectability (10%) no multinuclear uranyl complexes are sorbed

If we combine both the U—O and U—Fe distances obtained from our fits to samples UF4 and UF3 a model of the adsorption complex can be assembled that is self consistent By taking the shared edge length between the uranyl ion and the Fe oxyhydroxyl group as 3 0 A the observed U—Fe distance of 3 37 A (average) and assuming a mean Fe—O bond distance of 2 00 A we obtain the U—O equatorial distances at the adsorption bond of 2 51 A as observed Hence both this distance and the U—Fe distance support

Table 2 Summary of EXAFS Analysis[a]

Filtered fit results					Full EXAFS fitting			
Sample UF 4								
	U O_{ax}	U-O_{eq1}	U-$O_{eq2orbrg}$	U Fe	U O_{ax}	U O_{eq1}	U $O_{eq2orbrg}$	U Fe
N[b]	2 00	3 00	2 00	0 42	2 00	3 00	2 00	1 08
R(Å)[c]	1 79	2 34	2 46	3 33	1 80	2 35	2 52	3 41
σ^2 (Å^2)	0 002	0 0092	0 021	0 002	0 0028	0 0081	0 0084	0 009
E_0 (eV)	3 01	-3 01	-3 01	10 1	0 9	0 9	0 9	4 2
Sample UF3								
N[b]					2 00	3 00	2 00	1 04
R(Å)[c]					1 80	2 34	2 52	3 44
σ^2 (Å^2)					0 0024	0 0074	0 0062	0 0082
E_0 (eV)					2 66	2 66	2 66	1 95

[a]U O fits were made with integral coordination numbers i e all reasonable combinations of integral values were first attempted and those that resulted in best fits were fixed in subsequent refinements U Fe coordination numbers were floated in all fits

[b]Average coordination number

[c]Average bond distance

a mononuclear bidentate complex sharing an edge with a Fe oxyhydroxyl octahedron at the ferrihydrite crystallite edge (Fig. 10). This was also concluded by MANCEAU et al. (1992), although these authors observed a somewhat larger number of U—Fe pairs.

We also collected data for samples at lower uranyl concentrations (UF2 and UF1, U/Fe molar ratios of 0.001 and 0.0004 respectively). Although the EXAFS from these samples were too poor for full fitting analysis, the EXAFS were similar to that from the UF3 and UF4 samples, thus suggesting similar adsorption complexes for all samples. It should be noted that other ions, e.g., arsenate, also form bidentate complexes on the ferrihydrite surface (WAYCHUNAS et al., 1993). However, in the case of arsenate, the complex involved two surface hydroxyls in a corner-sharing complex rather than the edge-sharing complex described here.

Surface Complexation Modeling

Surface complexation modeling of the U(VI) adsorption data was developed with the diffuse double layer model (STUMM et al., 1970; HUANG and STUMM, 1973). In the diffuse double layer model, as in other surface complexation models, the surface is considered to be composed of specific functional groups that react with dissolved solutes to form coordinative complexes or ion pairs in a manner analogous to complexation reactions in solution (DAVIS and KENT, 1990). The effect of electrostatic charge at the ferrihydrite surface on the apparent strength of binding of charged ions in the model is calculated from the Gouy-Chapman theory for the electrical double layer by considering one layer of surface charge and a diffuse layer of counter charges in solution (DZOMBAK and MOREL, 1990). A surface area of 600 m^2 of $Fe_2O_3 \cdot H_2O$ was used in the model as recommended by DAVIS and LECKIE (1978) and DZOMBAK and MOREL (1990).

The modeling approach considered the simplest stoichiometry and number of reactions possible that was consistent with the EXAFS results and that would describe the experimental data. The process was begun by considering the simplest reaction possible with a one-site, bidentate surface complex, i.e.

$$\equiv Fe(OH)_2 + UO_2^{2+} = (\equiv FeO_2)UO_2^{+} + 2H^+, \quad (5)$$

where ($\equiv Fe(OH)_2$) represents the two surface hydroxyls forming an edge-sharing, bidentate surface complex with the uranyl ion (Fig. 10). Model calculations discussed below that consider this species only are referred to as Model 1. To constrain the modeling exercise initially, only U(VI) adsorption data in weakly acidic solutions (pH < 6) were considered because adsorption was essentially independent of the partial pressure of CO_2 in that range (Fig. 6). To test the goodness-of-fit for any proposed set of reactions, we applied the nonlinear, least-squares optimization program, FITEQL (WESTALL, 1982). FITEQL can adjust the values of one or two unknown surface complex formation constants in a chemical equilibrium model to yield the best fit of the reaction set to experimental data. FITEQL output includes the value of a goodness-of-fit parameter, SOS/DF, the sum of squares of the difference in value between model calculations and experimental data points divided by the degrees of freedom. A better fit to the experimental data yields a smaller value of SOS/DF when comparing an equal number of data points with the same relative or absolute error (FITEQL input parameters). Ideally, SOS/DF should approach a value of 1 before a model is considered valid (WESTALL, 1982).

In the initial calculations using Eqn. 5, we used the surface site density (0.205 mol sites/mol Fe in ferrihydrite) and acidity constant values that were recommended by DZOMBAK and MOREL (1990). All the U(VI) adsorption data as a function of U(VI) concentration for pH < 6 were considered simultaneously in the FITEQL runs. However, as shown in Fig. 11a, this one-site, one-species model produced a relatively poor fit to the data (SOS/DF = 46.4). Equation 5 was also tried with only one proton released per U(VI) adsorbed, but this produced an even poorer fit to the data (SOS/DF = 82.9).

Freundlich adsorption isotherms are usually observed for cation adsorption on ferrihydrite (BENJAMIN and LECKIE, 1981) and, as shown by KINNIBURGH (1986) and DZOMBAK and MOREL (1990), such adsorption data can be satisfactorily described by a two-site binding model. In a two-site model it is assumed that a small population of high-affinity sites exists on the surface, randomly distributed among a larger population of relatively low-affinity sites. Using this type of model combined with the diffuse double-layer model for electrostatic correction, DZOMBAK and MOREL (1990) compiled a set of adsorption constants for cation adsorption on ferrihydrite with the following reactions types:

$$Fe_sOH^0 + M^{2+} = Fe_sOM^+ + H^+ \quad (6)$$

and

$$Fe_wOH^0 + M^{2+} = Fe_wOM^+ + H^+ \quad (7)$$

where Fe_sOH^0 and Fe_wOH^0 represent strong-binding (high-affinity) and weak-binding (low-affinity) sites, respectively, and M^{2+} is a divalent cation. The electrical potential at the surface is assumed to be uniform, that is, of equal value at strong- and weak-binding sites.

To improve the fit of the model simulations to the U(VI) adsorption, the following bidentate reactions were considered for strong- and weak-binding sites:

$$(\equiv Fe_s(OH)_2) + UO_2^{2+} = (\equiv Fe_sO_2)UO_2^0 + 2H^+ \quad (8)$$

and

$$(\equiv Fe_w(OH)_2) + UO_2^{2+} = (\equiv Fe_wO_2)UO_2^0 + 2H^+ \quad (9)$$

Initial calculations using Eqns. 8 and 9 (the two-site Model 1) were performed with the site densities for strong- and weak-binding sites that were recommended by DZOMBAK and MOREL (1990), i.e., 5 mmol strong sites/mol Fe and 0.2 mol weak sites/mol of Fe. The agreement between the model simulations and experimental data was improved (SOS/DF = 24.2), but characteristics of the model simulations suggested that considerable improvement could be obtained by changing the values of the site densities. For example, the model was unable to simulate the observed differences in fractional adsorption for total U(VI) concentrations of

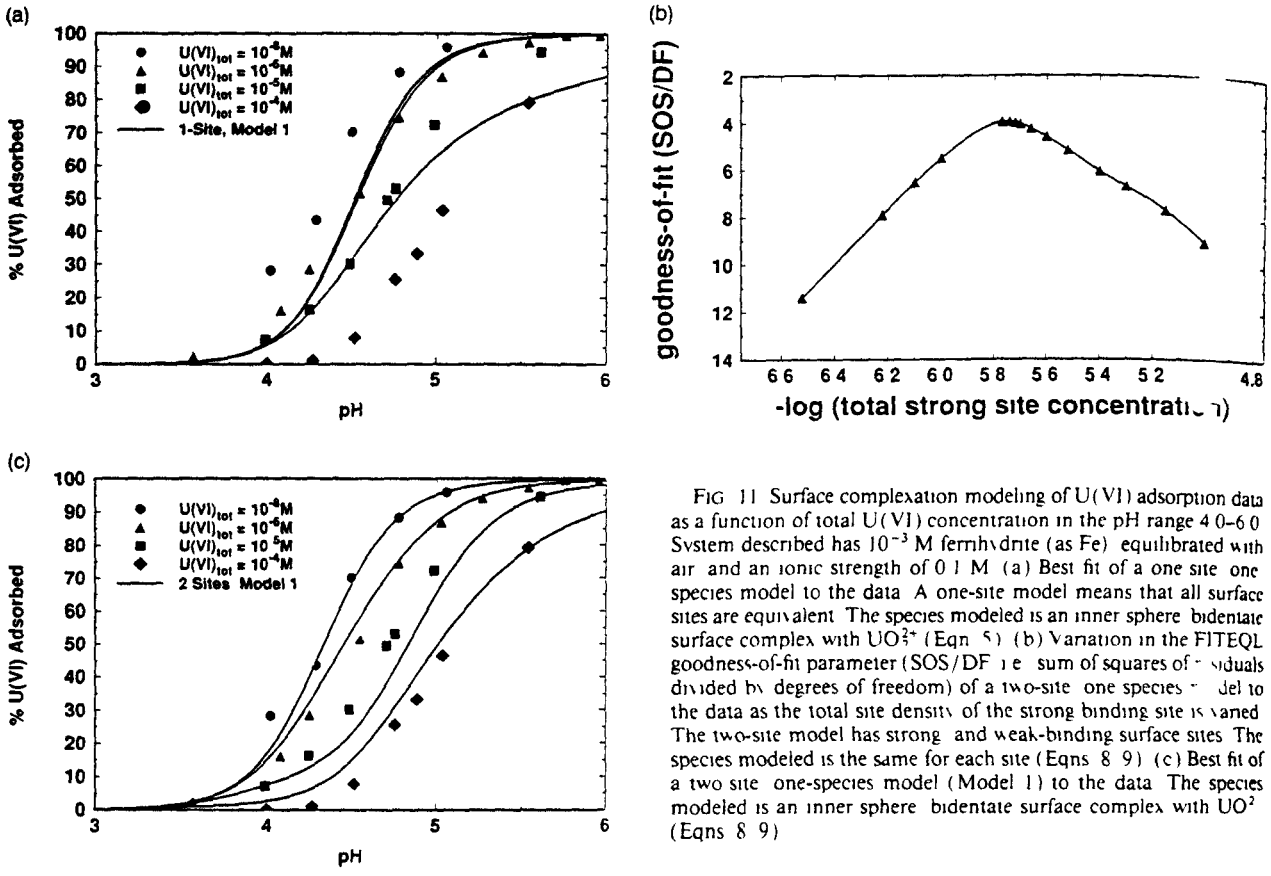

FIG 11 Surface complexation modeling of U(VI) adsorption data as a function of total U(VI) concentration in the pH range 4.0–6.0. System described has 10^{-3} M ferrihydrite (as Fe) equilibrated with air and an ionic strength of 0.1 M. (a) Best fit of a one site one species model to the data. A one-site model means that all surface sites are equivalent. The species modeled is an inner sphere bidentate surface complex with UO_2^{2+} (Eqn 5). (b) Variation in the FITEQL goodness-of-fit parameter (SOS/DF i.e. sum of squares of residuals divided by degrees of freedom) of a two-site one species model to the data as the total site density of the strong binding site is varied. The two-site model has strong and weak-binding surface sites. The species modeled is the same for each site (Eqns 8, 9). (c) Best fit of a two site one-species model (Model 1) to the data. The species modeled is an inner sphere bidentate surface complex with UO_2^{2+} (Eqns 8, 9).

10^{-8} M and 10^{-6} M because the strong sites (5×10^{-6} M) were in excess for both cases. To model the difference observed in the experimental data requires a strong-site concentration that approaches saturation in the system with 10^{-6} M U(VI). In addition, the adsorption data at 10^{-4} M total U(VI) were poorly described because of weak site saturation.

To improve agreement between the model and experimental data, the following steps were taken: (1) the strong-binding site density was determined by optimization with FITEQL as discussed below and (2) the total site density was set to 0.875 mol sites/mol Fe. Since the surface complex is bidentate, 2×10^{-4} M sites are required to adsorb 10^{-4} M U(VI). The total number of sites in the previous calculations was only 2.05×10^{-4} M. A higher number of surface functional groups for the weak-binding site density is supported by tritium exchange studies (YATES 1975, DAVIS 1977), experimental adsorption data for arsenate (FULLER et al., 1993), geometric considerations for primary particles composed of short double Fe octahedral chains (WAYCHUNAS et al., 1993), and previous surface complexation modeling applications to ferrihydrite (DAVIS et al. 1978, DAVIS and LECKIE 1978, 1980, ZACHARA et al. 1987). Although optimization of the weak-binding site density is also possible in principle, the process is more cumbersome because the acidity constants and other adsorption constants must be rederived each time a new total site density is chosen (see DAVIS and KENT 1990 for a discussion of why the constants depend on the site density). For all calculations discussed below, the acidity and carbonate adsorption constants that were used are given in Table 3. These values were determined with FITEQL and are consistent with a total site density of 0.875 moles sites/mol Fe. Acidity constants were not rederived each time that the strong site density was changed since it was assumed that the acidity of weak and strong sites was identical (DZOMBAK and MOREL 1990). Carbonate adsorption constants were included because it has been demonstrated that carbonate can adsorb on Fe oxides (VAN GEEN et al. 1994, ZACHARA et al. 1987, BRUNO et al. 1992).

Using Eqns 8 and 9 to describe U(VI) adsorption, FITEQL was run in an iterative fashion with the strong-binding site density as a variable. Each run produced a different value of the goodness-of-fit parameter allowing an estimate of an optimal value for the strong-binding site density of 1.8 mmol sites/mol Fe for the two-site Model 1 (Fig. 11b). Using this value for the strong-binding site density gave a substantially better fit (SOS/DF = 4.0) to the adsorption data for this two-site one-species model (Fig. 11c). Stability constants for the two U(VI) adsorption reactions are given in Table 3. As mentioned above, carbonate adsorption reactions were included in the modeling but these reactions had a negligible effect on the simulations of U(VI) adsorption in this pH range at a partial pressure of CO_2 of $10^{-3.5}$. The fit to the data at 10^{-4} and 10^{-5} total U(VI) concentration could only be improved by adding a third type of surface site to the model which was considered unwarranted.

The FITEQL modeling described above was performed by

Table 3 Ferrihydrite Surface Reactions[a]

Reaction	log K (I=0 1)	Note
$\equiv FeOH + H^+ = \equiv FeOH_2^+$	6 51	b
$\equiv FeOH = \equiv FeO^- + H^+$	9 13	b
$\equiv FeOH + H_2CO_3^\circ = \equiv FeCO_3H^\circ + H_2O$	2 90	c
$\equiv FeOH + H_2CO_3^\circ = \equiv FeCO_3^- + H_2O + H^+$	5 09	c
$(\equiv Fe_s(OH)_2) + UO_2^{2+} = (\equiv Fe_sO_2)UO_2^\circ + 2H^+$	2 57	d f
$(\equiv Fe_w(OH)_2) + UO_2^{2+} = (\equiv Fe_wO_2)UO_2^\circ + 2H$	6 28	d f
$(\equiv Fe_s(OH)_2) + UO_2^{2+} + CO_3^{2-} = (\equiv Fe_sO_2)\,UO_2CO_3^{2-} + 2H$	3 67	e f
$(\equiv Fe_w(OH)_2) + UO_2^{2+} + CO_3^{2-} = (\equiv Fe_wO_2)\,UO_2CO_3^{2-} + 2H$	0 42	e f

[a]All constants determined with FITEQL using a two site diffuse double layer model and a total site density of 0 875 moles sites/mole Fe

[b]From FITEQL fit of titration data of Davis (1977) Reaction constants for weak and strong surface sites assumed to be equal

[c]From FITEQL fit of carbonate adsorption data of Zachara et al (1987) for the closed system (C_T= 4 6 x 10^{-6}M, Fe_T=8 7 x 10^{-4}M 0 1 M $NaNO_3$) Reaction constants for weak and strong surface sites assumed to be equal

[d]From FITEQL fit of U(VI) adsorption data as a function of total U(VI) concentration in the pH range 4 0 6 0 with a strong site density of 0 0018 moles sites/ mole Fe

[e]From FITEQL fit of U(VI) adsorption data at I=0 1 in the pH range 6 5 9 (after determining constants for data in the pH 4 6 range)

[f]Mass action equations with bidentate surface complexes are defined with an exponent of one for ≡FeOH However mass balance equations assume a stoichiometric coefficient of two for ≡FeOH (consuming two sites) following the approach of Davis and Leckie (1980) Calculations with differing coefficients for the mass action and mass balance equations are possible with FITEQL, but not with HYDRAQL

fitting all of the adsorption data where pH was less than 6 To test the robustness of the model at higher pH values where carbonate complexation is important the same stability constants for Eqns 8 and 9 (Table 3) were applied in simulations of U(VI) adsorption data in alkaline solutions at two partial pressures of CO_2 (Fig 12a) Adsorption of U(VI) was slightly underpredicted by the simulations in the higher pH range with the degree of underprediction increasing with increasing partial pressure of CO_2 However the predictions were actually quite good for a one species model considering the range of conditions and the complexity of previous surface speciation models published for this system

To determine whether a simple refinement of the model would result in even better agreement with the data a two-site two-species model (Model 2) was tested where the second species proposed was a ternary surface complex composed of the two edge-sharing surface hydroxyls the uranyl cation and a carbonate anion i e

$$(\equiv Fe_s(OH)_2) + UO_2^{2+} + CO_3^{2-} = (\equiv Fe_sO_2)UO_2CO_3^{2-} + 2H^+ \quad (10)$$

and

$$(\equiv Fe_w(OH)_2) + UO_2^{2+} + CO_3^{2-} = (\equiv Fe_wO_2)UO_2CO_3^{2-} + 2H^+ \quad (11)$$

The stability constants for the reactions shown in Eqns 10 and 11 (see Table 3) were determined with FITEQL by fitting U(VI) adsorption data at an ionic strength of 0 1 M in the pH range 6 5–9 0 The same constants for Eqns 8 and 9 were used as determined previously in Model 1 The Model 2 simulations in the alkaline pH range are in excellent agreement with the data (Fig 12a) A similar result has been observed by KOHLER et al (1995) in a study of U(VI) adsorption by goethite Interestingly the slight shift of the Model 2 simulations to predict more U(VI) adsorption near pH 4 75 at the higher partial pressure of CO_2 is consistent with the experimental data Although the difference in predicted U(VI) adsorption between Models 1 and 2 in the alkaline pH range is small the ternary surface complex is predicted to be the most important surface species in the pH range 6–9 (Fig 12b) The model simulations suggest that it would only be a minor surface species near pH 5, at which samples for

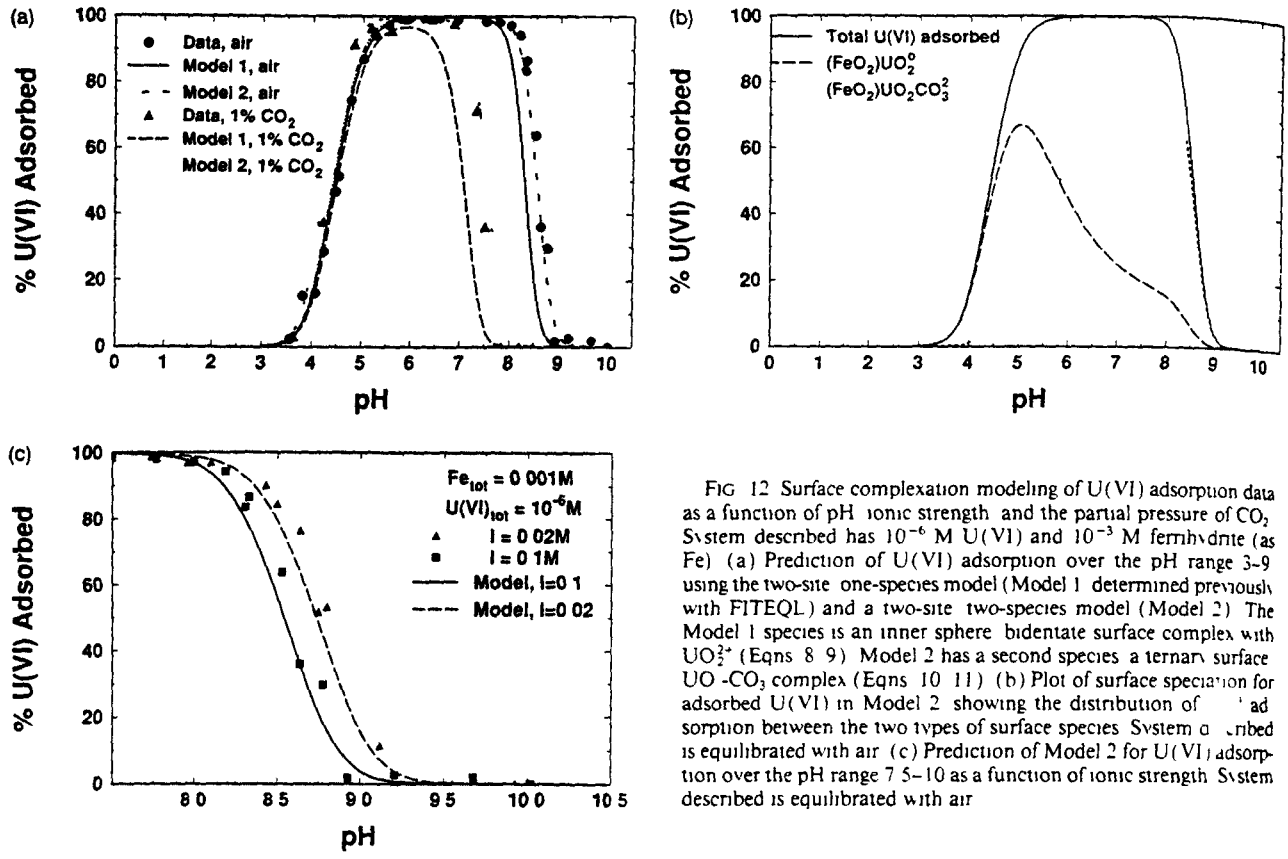

FIG 12 Surface complexation modeling of U(VI) adsorption data as a function of pH ionic strength and the partial pressure of CO_2 System described has 10^{-6} M U(VI) and 10^{-3} M ferrihydrite (as Fe) (a) Prediction of U(VI) adsorption over the pH range 3–9 using the two-site one-species model (Model 1 determined previously with FITEQL) and a two-site two-species model (Model 2) The Model 1 species is an inner sphere bidentate surface complex with UO_2^{2+} (Eqns 8 9) Model 2 has a second species a ternary surface UO -CO_3 complex (Eqns 10 11) (b) Plot of surface speciation for adsorbed U(VI) in Model 2 showing the distribution of ad sorption between the two types of surface species System described is equilibrated with air (c) Prediction of Model 2 for U(VI) adsorption over the pH range 7 5–10 as a function of ionic strength System described is equilibrated with air

EXAFS analysis were prepared The ternary surface complex which is negatively charged (Eqns 10, 11) may account for the observed charge reversal of iron oxide particles after adsorption of U(VI) in the presence of carbonate as reported by HO and MILLER (1986)

The model simulations also agree well with the dependence of U(VI) adsorption on ionic strength in the pH 8–9 5 range (Fig 12c) The ionic strength dependence of U(VI) adsorption in this pH range does not mean that the ternary surface complex formed is necessarily an outer-sphere species The diffuse double layer model used considers only inner-sphere surface complexes (DZOMBAK and MOREL, 1990) Instead, the ionic strength dependence of calculated adsorption in this pH range derives from the change in activities of the dominant aqueous species of U(VI), the highly charged carbonato complexes (Fig 2a)

The modeling results suggest that the surface speciation of U(VI) may be far simpler than that observed in aqueous solution As shown by the EXAFS results the coordination environment at the surface may give strong preference to the bidentate edge-sharing linkage that is stable over a wide pH range In the alkaline pH range, carbonate may then attach to adsorbed uranyl ion to form the ternary surface complex, although the results do not reveal any structural information about the complex It appears unlikely that aqueous species such as $UO_2(CO_3)_2^{2-}$ or $UO_2(CO_3)_3^{4-}$ would adsorb strongly at the Fe oxide surface as proposed by HSI and LANGMUIR (1985) due to steric and coordinative constraints Instead the data suggest that at the pH values at which these species become predominant in aqueous solution (pH > 8 in air, pH > 7 in 1% CO_2 see Fig 2) U(VI) is desorbed from the ferrihydrite surface (Fig 12a)

CONCLUSIONS

Major findings of the experimental and modeling studies of U(VI) adsorption on ferrihydrite are noted below

(1) EXAFS analysis and the trend in U(VI) adsorption on ferrihydrite as a function of U(VI) concentration suggest that polynuclear U(VI) species do not form readily at the surface in the circumneutral pH range as they do in solution

(2) The experimental data EXAFS analysis, and model simulations suggest that the major U(VI) species at the ferrihydrite surface in the acidic pH range is an inner sphere bidentate complex involving two surface hydroxyls of an Fe octahedron edge and the uranyl cation

(3) A diffuse double-layer two-site surface complexation model with two proposed surface species provides an excellent description of U(VI) adsorption on ferrihydrite over a wide range of pH, U(VI) concentration and two CO_2 partial pressures Manipulation of strong- and weak-binding site densities was necessary in order to obtain the best agreement between data and model simulations Compared to the site densities recommended for ferrihydrite by DZOMBAK and MOREL (1990) decreasing the strong-site density by a factor of 3 and increasing the

weak-site density by a factor of 4 greatly improved the model simulations as a function of U(VI) concentration

(4) The coordination environment of the ferrihydrite surface may limit the complexity of U(VI) surface speciation in comparison to that observed in aqueous solution. Binding of the 1:1 uranyl-carbonate complex at the surface is suggested from the results of batch adsorption studies and associated surface complexation modeling, however coordination of U(VI) with two or more carbonate ligands may prevent surface coordination.

Acknowledgments—The authors thank the U.S. Nuclear Regulatory Commission for partial funding of this study. The EXAFS analysis benefited from many helpful discussions with H. A. Thompson on the use of FEFF and U-compound spectra fitting. Uranium model compound spectra collected by Ms. Thompson as part of another study were vital for testing calculated phase and amplitude functions. J. Westall assisted on several occasions on the best approaches for using FITEQL. The authors thank C. Fuller and L. Anderson for thoughtful reviews of the manuscript. C. Fuller for assistance with EXAFS data collection and M. Kohler and D. Kent for discussions and interest in surface complexation modeling.

Editorial handling: G. Rich Holdren Jr.

REFERENCES

ABERG M. (1969) The crystal structure of $[(UO_2)_3(OH)_2Cl_2(H_2O)_4]$. *Acta Chem. Scand.* **23**, 791–810.

ABERG M. (1970) On the structures of the predominant hydrolysis products of uranyl(VI) in solution. *Acta Chem. Scand.* **24**, 2901–2915.

ABERG M. (1971) On the crystal structure of a tetranuclear hydroxo complex of uranyl(VI). *Acta Chem. Scand.* **25**, 368–369.

ÅBERG M., FERRI D., GLASER J. and GRENTHE I. (1983) Studies of metal carbonate equilibria. 8. Structure of the hexakis(carbonato)tris[dioxouranate(VI)] ion in aqueous solution. An X-ray diffraction and ^{13}C NMR study. *Inorg. Chem.* **22**, 3981–3985.

BENJAMIN M. M. and LECKIE J. O. (1981) Multiple-site adsorption of Cd, Cu, Zn, and Pb on amorphous iron oxyhydroxide. *J. Colloid Interface Sci.* **79**, 209–221.

BROWN G. E. (1990) Spectroscopic studies of chemisorption reaction mechanisms at oxide-water interfaces. In *Mineral Water Interface Geochemistry* (ed. M. F. HOCHELLA and A. F. WHITE). *Rev. Mineral. 23*, pp. 309–363.

BRUNO J., STUMM W., WERSIN P. and BRANDBERG F. (1992) On the influence of carbonate in mineral dissolution. Part I. The thermodynamics and kinetics of hematite dissolution in bicarbonate solutions at $T = 25°C$. *Geochim. Cosmochim. Acta* **56**, 1139–1148.

CHISHOLM-BRAUSE C., HAYES K. F., ROE L. A., BROWN G. E., PARKS G. A. and LECKIE J. O. (1990) Structure of Pb(II) complexes at the γ-Al_2O_3/water interface. *Geochim. Cosmochim. Acta* **54**, 1897–1909.

COMBES J.-M. (1988) Evolution de la structure locale des polymeres et gels ferriques lors de la cristallisation des oxides de fer. Application au piegeage de l'uranium. Thesis, Univ. Paris 7.

DAVIS J. A. (1977) Adsorption of Trace Metals and Complexing Ligands at the Oxide/Water Interface. Ph.D. thesis, Stanford Univ.

DAVIS J. A. and KENT D. B. (1990) Surface complexation modelling in aqueous geochemistry. In *Mineral-Water Interface Geochemistry* (ed. M. F. HOCHELLA and A. F. WHITE). *Rev. Mineral. 23*, pp. 7–260.

DAVIS J. A. and LECKIE J. O. (1978) Surface ionization and complexation at the oxide/water interface. II. Surface properties of amorphous iron oxyhydroxide and adsorption of metal ions. *J. Colloid Interface Sci.* **67**, 90–107.

DAVIS J. A. and LECKIE J. O. (1980) Surface ionization and complexation at the oxide/water interface. III. Adsorption of anions. *J. Colloid Interface Sci.* **74**, 32–43.

DAVIS J. A., JAMES R. O. and LECKIE J. O. (1978) Surface ionization and complexation at the oxide/water interface. I. Computation of electrical double layer properties in simple electrolytes. *J. Colloid Interface Sci.* **63**, 480–499.

DOUSMA J. and DE BRUYN P. L. (1976) Hydrolysis-precipitation studies of iron solutions. I. Model for hydrolysis and precipitation from Fe(III) nitrate solutions. *J. Colloid Interface Sci.* **56**, 527–539.

DZOMBAK D. A. and MOREL F. M. M. (1990) *Surface Complexation Modelling: Hydrous Ferric Oxide*. Wiley.

FULLER C. C., DAVIS J. A. and WAYCHUNAS G. A. (1993) Surface chemistry of ferrihydrite. 2. Kinetics of arsenate adsorption and coprecipitation. *Geochim. Cosmochim. Acta* **57**, 2271–2282.

GRENTHE I. et al. (1992) *Chemical Thermodynamics of Uranium*. Elsevier.

HO C. H. and DOERN D. C. (1985) The sorption of uranyl species on a hematite sol. *Canadian J. Chem.* **63**, 1100–1104.

HO C. H. and MILLER N. H. (1986) Adsorption of uranyl species from bicarbonate solution onto hematite particles. *J. Colloid Interface Sci.* **110**, 165–171.

HSI C. D. and LANGMUIR D. (1985) Adsorption of uranyl onto ferric oxyhydroxides: Application of the surface complexation site binding model. *Geochim. Cosmochim. Acta* **49**, 1931–1941.

HUANG C. P. and STUMM W. (1973) Specific adsorption of cations on hydrous α-Al_2O_3. *J. Colloid Interface Sci.* **22**, 231–259.

KOHLER M., HONEYMAN B. D. and LECKIE J. O. (1995) Uranyl interactions in the goethite/solution interphase: region formation of binary and ternary surface complexes (in prep.).

KINNIBURGH D. G. (1986) General purpose adsorption isotherms. *Environ. Sci. Tech.* **20**, 895–904.

MANCEAU A., COMBES J. M. and CALAS G. (1990) New data and a revised structural model for ferrihydrite. Comment. *Clays Clay Mineral.* **38**, 331–334.

MANCEAU A., CHARLET L., BOISSET M. C., DIDIER B. and SPANDINI L. (1992) Sorption and speciation of heavy metals on hydrous Fe and Mn oxides. From microscopic to macroscopic. *Appl. Clay Sci.* **7**, 201–223.

MURPHY P. J., POSNER A. M. and QUIRK J. P. (1976a) Characterization of partially neutralized ferric chloride solutions. *J. Colloid Interface Sci.* **56**, 284–298.

MURPHY P. J., POSNER A. M. and QUIRK J. P. (1976b) Characterization of hydrolyzed ferric ion solutions. *J. Colloid Interface Sci.* **56**, 312–319.

MUSTRE DE LEON J., RHER J. J., ZABINSKY S. I. and ALBERS R. C. (1991) Ab initio curved-wave x-ray absorption fine structure. *Phys. Rev.* **B44**, 4146–4156.

PAPELIS C., HAYES K. F. and LECKIE J. O. (1988) *HYDRAQL: A Program for the Computation of Aqueous Batch Systems Including Surface Complexation Modeling of Ion Adsorption at the Oxide/Solution Interface*. Tech. Rept. 306, Dept. of Civil Eng., Stanford University.

PAYNE T. E. and WAITE T. D. (1991) Surface complexation modelling of uranium sorption data obtained by isotope exchange techniques. *Radiochim. Acta* **52/53**, 487–493.

REA B. A., DAVIS J. A. and WAYCHUNAS G. A. (1994) Studies of the reactivity of the ferrihydrite surface by iron isotopic exchange and Mossbauer spectroscopy. *Clays Clay Mineral.* **42**, 23–34.

REHR J. J., MUSTRE DE LEON J., ZABINSKY S. I. and ALBERS R. C. (1991) Theoretical X-ray absorption fine structure standards. *J. Amer. Chem. Soc.* **113**, 5135–5140.

ROE L. A. et al. (1991) In situ X-ray absorption study of lead ion surface complexes. *Langmuir* **7**, 367–373.

SAGERT N. H., HO C. H. and MILLER N. H. (1989) The adsorption of uranium(VI) onto a magnetite sol. *J. Colloid Interface Sci.* **130**, 283–287.

SCHWERTMANN U. and FISCHER W. R. (1973) Natural amorphous ferric hydroxide. *Geoderma* **10**, 237–247.

SCHWERTMANN U. and TAYLOR R. M. (1977) Iron oxides. In *Minerals in Soil Environments* (ed. J. B. DIXON and S. B. WEED), pp. 145–180. Soil Sci. Soc. Amer.

STARIK I E, STARIK F E, and APPOLONOVA A N (1958) Adsorption of microquantities of uranium by iron hydroxides and its desorption by the carbonate method *J Inorg Chem USSR* **3**, 181–193

STERN E A and HEALD S M (1979) X-ray filter assembly for fluorescence measurements of X-ray absorption fine structure standards *Rev Sci Instr* **50**, 1579–1582

STUMM W HUANG C P, and JENKINS S R (1970) Specific chemical interactions affecting the stability of dispersed systems *Croat Chem Acta* **42**, 223–244

TOWE K M and BRADLEY W F (1967) Mineralogical constitution of colloidal "hydrous ferric oxides *J Colloid Interface Sci* **24**, 384–392

TRIPATHI V S (1983) Uranium transport modelling geochemical data and sub-models Ph D dissertation, Stanford Univ

VAN GEEN A ROBERTSON A P and LECKIE J O (1994) Complexation of carbonate species at the goethite surface Implications for adsorption of metal ions in natural waters *Geochim Cosmochim Acta* **58**, 2073–2086

WAITE T D, PAYNE T E DAVIS J A and SEKINE K (1994) *Uranium Sorption Alligator Rivers Analogue Proj Final Rept 13* Australian Nuclear Science and Technology Organisation

WAYCHUNAS G A REA B A FULLER C C and DAVIS J A (1993) Surface chemistry of ferrihydrite 1 EXAFS studies of the geometry of coprecipitated and adsorbed arsenate *Geochim Cosmochim Acta* **57**, 2251–2269

WAYCHUNAS G A FULLER C C REA B A and DAVIS J A (1995) Wide angle X-ray scattering (WAXS) study of two line ferrihydrite and the effects of arsenate sorption Comparison with EXAFS results *Geochim Cosmochim Acta* (submitted)

WESTALL J C (1982) FITEQL *A Program for the Determination of Chemical Equilibrium Constants from Experimental Data User's guide Version 2 0* Chemistry Department Oregon State Univ

YATES D E (1975) The structure of the oxide/aqueous electrolyte interface Ph D dissertation Univ Melbourne Australia

ZACHARA J M GIRVIN D C SCHMIDT R L and RESCH C T (1987) Chromate adsorption on amorphous iron oxyhydroxy in the presence of major groundwater ions *Environ Sci Tec* **21**, 589–594

14/14